THE ASTROPHYSICAL JOURNAL, 367:239–252, 1991 January 20

EVOLUTIONARY MODELS OF HALO STARS WITH ROTATION. I. EVIDENCE FOR DIFFERENTIAL ROTATION WITH DEPTH IN STARS

MARC H. PINSONNEAULT, CONSTANTINE P. DELIYANNIS[1], AND PIERRE DEMARQUE
Center for Solar and Space Research, Center for Theoretical Physics, and Department of Astronomy, Yale University
Received 1990 June 8; accepted 1990 July 16

ABSTRACT

We have computed evolutionary models of metal-poor stars including the effects of rotation, and we have compared their properties with observations. The models rotate slowly at the surface, in agreement with the observed upper limits on the rotation velocity at main-sequence turnoff; they also have substantial differential rotation with depth. This differential rotation preserves a sufficient amount of internal angular momentum to explain the rapid rotation of evolved horizontal-branch stars. These results hold for a wide range of angular momentum loss and transport parameter values. Differences and similarities between the surface and internal rotation of solar metallicity and metal-poor models are discussed. Rigidly rotating models are found to be incompatible with the observations once giant branch mass loss is taken into account. More stringent upper limits on main-sequence rotation velocities (at the 3 km s^{-1} level) would rule out rigidly rotating main-sequence models even without accounting for post-main sequence mass loss. Horizontal-branch rotation velocity measurements as a function of color are proposed as a test of the rotation law enforced in convection zones, and their dependence on cluster age and metallicity are discussed.

Subject headings: stars: evolution — stars: horizontal-branch — stars: interiors — stars: Population II — stars: rotation

I. INTRODUCTION

Stellar rotation is an important property that can induce changes in the structure and evolution of stars which are directly or indirectly observable. It also provides an additional diagnostic, in the form of stellar rotation rates as a function of mass, age, and composition, to supplement the other observable quantities used to test standard stellar evolution theory.

Rotation also induces motions which cause material mixing. Meridional circulation currents, which are a necessary consequence of stellar rotation (Eddington 1925; Kippenhahn and Möllenhoff 1974; Tassoul and Tassoul 1982), cause steady mixing. Schatzman (1969) was the first to note that turbulence induced by rotation could also produce mixing. Subsequent work indicated that in the presence of angular velocity gradients, instability mechanisms capable of producing substantial mixing could be triggered (Knobloch and Spruit 1982; Zahn 1983, 1987). There is observational evidence that mixing beyond that present in standard stellar models occurs in evolved stars (Smith 1987; Suntzeff 1989; see also Deliyannis, Demarque, and Pinsonneault 1989, hereafter DDP; Pinsonneault, Deliyannis, and Demarque 1990, hereafter PDD, and references therein). Rotationally induced mixing is also an appealing explanation for the observed depletion of surface light element abundances in the Sun (Pinsonneault *et al.* 1989, hereafter PKD; see also Baglin, Morel, and Schatzman 1985; cluster stars (Pinsonneault, Kawaler, and Demarque 1990, hereafter PKD; see also Baglin, Morel, and Schatzmann 1985; Vauclair 1988; Charbonneau and Michaud 1990), and metal-poor stars (PDD; see also Vauclair 1988). Stellar rotation also provides information about such important stellar properties as age (PKD; Kawaler 1989) which is otherwise difficult to obtain.

However, incorporating the effects of rotation in stellar evolution makes the problem substantially more difficult. There are theoretical uncertainties in the evolution of the angular momentum distribution (e.g., Tassoul 1978), and until recently there were too few observations to adequately constrain the theory. *By studying stars of different age, mass, and composition the theoretical properties of stellar models with rotation can be usefully constrained, and a consistent theory can be applied to a wide variety of stars.*

In previous papers, we have constructed evolutionary models that include rotation for the Sun (PKSD) and open cluster stars (up to an age of 1.7 Gyr) of a variety of ages and masses (PKD). The Sun provides a valuable zero point for calibration of the angular momentum loss law and the efficiency of material mixing. We required that any choice of model rotational parameters be capable of reproducing the solar rotation rate and surface lithium abundance at the solar age. The rotation of open cluster stars with ages less than 1.7 Gyr was found to constrain both the time dependence of the angular momentum loss law and the time scale for internal angular momentum redistribution.

The lack of information on the internal rotation of stars has been the single most important uncertainty in the construction of stellar models with rotation. We have already derived constraints on differential rotation with depth in both the solar and open cluster models. However, main-sequence models can provide only indirect evidence about the internal rotation of stars. By contrast, *evolved stars provide a direct test of the internal rotation of their main-sequence progenitors.*

The detection of substantial rotation in field horizontal-branch stars by Peterson, Tarbell, and Carney (1983) and in globular cluster horizontal branch stars by Peterson (1983; 1985*a*, *b*) has important implications for the internal rotation of stars. The inferred masses of horizontal branch stars in globular clusters are substantially lower than the inferred turnoff masses of the clusters. This requires $\sim 0.15\ M_{\odot}$ of mass loss during the giant branch phase of evolution (Faulkner 1966; Hartwick, Härm, and Schwarzschild 1968; Rood 1970,

[1] Also at Department of Physics, Yale University.

1973; Demarque and Mengel 1971, 1972; Reimers 1975 and references therein; Sweigart and Gross 1976; Lee, Demarque, and Zinn 1990, hereafter LDZ). *Material at the surface of a horizontal-branch star was therefore well below the surface of the main-sequence progenitor, and a comparison of the rotation of horizontal-branch stars with the rotation of stars at the main-sequence turnoff serves as a probe of the internal rotation of main-sequence stars.* Some of the implications of the horizontal-branch observations have been discussed by Peterson (1983), Endal (1987), PKSD, and DDP. Because of the importance of the results, we present a detailed analysis in this paper.

Halo stars also provide an important test of main-sequence rotation properties in a very different regime of age and metallicity than the open cluster stars. For example, they provide a potential test for the validity of the angular momentum loss law for low-mass stars. Low-mass Population I stars rotate slowly at their surface by an age of 10^9 yr. If halo stars experience comparable angular momentum loss they too should rotate slowly, especially given their much greater ages. For open cluster stars, solar calibrated models can reproduce the observed rotation velocities and abundances as a function of mass and age (PKD). Halo star models can be used to test the applicability of the solar calibration to halo stars.

In contrast to the case of open cluster stars, there is little information on the main sequence rotation of halo stars (§ III). The observed slow main-sequence rotation requires angular momentum loss on the main sequence; the current observational limits by themselves, however, require neither the same degree of angular momentum loss as seen in Population I stars nor the same history. The only reasonable approach is therefore to apply different angular momentum loss laws (appropriate for Population I stars) to metal-poor models, and to see what happens. We will show that an extremely inefficient angular momentum loss law would be needed to preserve any significant surface rotation rate in such old stars. We also note that there is no theoretical reason to expect such a different angular momentum loss law in Population II stars.

For the open cluster star models the range of initial angular momenta were derived from extrapolation of the relationship between total angular momentum and mass for massive Population I stars (Kawaler 1987) and from the angular momenta inferred from T Tauri stars (Hartmann and Stauffer 1989). We have no comparable source of information about the initial angular momenta of halo stars. We therefore assume the same range of initial angular momenta for halo stars that we used for models of open cluster stars of the same mass (PKD). As we will show, there is no observational evidence for a substantially different range of initial angular momenta; furthermore, only extremely low initial angular momenta would significantly alter our conclusions.

Finally, we can test the angular momentum redistribution time scales and stability conditions in the metal-poor context, again using the solar calibration. Given the ability of the solar calibrated models to reproduce open cluster observations of stars with different masses and ages, this is a reasonable procedure. We can then pose a simple question: can the observed properties of halo stars be reproduced with the same physical assumptions used to reproduce the solar and open-cluster star observations?

II. METHOD

The approach we use for constructing stellar models with rotation follows the philosophy of the pioneering work of Endal and Sofia (1978, 1981). For a description of the implementation in our stellar models see PKSD; Pinsonneault (1988) contains a detailed description of the numerical techniques. We begin on the Hayashi track with a fully convective pre–main-sequence model. Rigid rotation is enforced in convective regions; the assumed initial angular momentum is therefore sufficient to specify the initial angular momentum distribution. We then evolve the model to the desired age, applying angular momentum loss from a magnetic wind to the surface convection zone. The angular momentum loss model is calibrated to reproduce the observed spindown of solar metallicity main sequence stars.

Angular velocity gradients will be generated in the models, both at the base of the surface convection zone (by angular momentum loss) and by evolutionary structural changes. These gradients can be unstable, leading to redistribution of angular momentum and material mixing. Internal redistribution of angular momentum by meridional circulation and rotationally induced instabilities, and the associated material mixing, are treated by coupled diffusion equations. The constant in the angular momentum loss expression and the efficiency of material mixing relative to angular momentum redistribution are adjusted to reproduce the solar rotation rate and surface lithium depletion at the solar age.

For our basic case we used the standard set of rotation parameters from the open cluster paper (case A in PKD). The angular momentum loss law of this basic case was chosen so that the surface rotation velocities of the models reproduce the empirical Skumanich (1972) $t^{-1/2}$ law spin-down at late ages.

From the observations of Population I stars, we know that stars of the same mass and age arrive on the main sequence with a range of initial angular momenta, J_0; cases with $\log J_0 = 49.2$, 49.7, and 50.2 (g cm^2 s^{-1}) cover the inferred range in J_0 for models of low-mass open cluster stars (PKD). Since there are no young Population II stars available, we use the same range for the metal-poor models studied in this paper. To compare these angular momenta with observations it is useful to define a critical angular momentum such that a rigid rotator is marginally bound at the equator on the surface. For the halo star models, the initial angular momenta we have chosen correspond to approximately one-half, one-sixth, and 1/20 of the critical angular momentum in the absence of angular momentum loss.

Because the observations span a range in metallicity we considered models with both $Z = 10^{-3}$ and $Z = 10^{-4}$. All models were computed with a helium abundance $Y = 0.24$ which is compatible with theoretical big bang nucleosynthesis arguments (Boesgaard and Steigman 1985) and observational evidence (Pagel and Simonson 1989). We chose a value for the model mixing length $\alpha = 1.4$ by requiring the solar model to have the solar radius at the age of the Sun (Guenther, Jaffe, and Demarque 1989).

To cover the observed range in effective temperature for the halo stars, we have run sequences with total masses (in solar mass units) of 0.5, 0.55, and 0.6–0.85 in increments of 0.025. Evolution of the lower mass models was terminated at an age of 20 Gyr. Some of the higher mass models evolved off the main sequence at earlier ages; for the purposes of this paper we will consider only the main-sequence properties of the models and defer a discussion of post-main sequence evolution to future papers.

We also considered different choices for angular momentum loss (cases B and C in PKD) and angular momentum transport. In addition, we varied the sensitivity of angular momen-

tum transport to mean molecular weight gradients (parameter F_μ in PKSD) and changes in the critical Reynolds number (cases F in PKD) to test for differences in the degree of core rotation.

III. PROPERTIES OF THE MODELS

In this paper we concentrate on comparing the surface and internal rotation of our models with observations of main sequence and evolved stars. Models with rotation also have different structural properties than standard models, and rotational mixing can alter the surface abundances of the models. The importance of the structural changes caused by rotation is discussed in DDP, and the main-sequence lithium depletion in metal-poor models with rotation is discussed in PDD. Other papers in progress will discuss implications for cosmology (Deliyannis, Pinsonneault, and Demarque 1990), beryllium depletion (Deliyannis and Pinsonneault 1990), lithium in subgiants (Pinsonneault and Deliyannis 1990), and main-sequence mixing of CNO process elements.

a) Observations of Rotation in Metal-Poor Stars

The surface rotation velocities of models with rotation can be directly compared with observations; the internal rotation of the models can also be compared with the rotation of evolved stars. For solar metallicity stars, we have observations of rotation velocities (and periods) for stars with a variety of ages, masses, and in different evolutionary states. We can therefore constrain important model properties, such as the time scale for transport of angular momentum from the surface to the interior, by comparing the models with the observations of Population I stars (PKD). For metal-poor stars, there are currently only upper limits on the surface rotation rate on the main sequence. Metal-poor stars therefore provide much weaker constraints on the main sequence rotation of the models than solar metallicity stars do.

However, the rotation of evolved metal-poor stars provides the best current constraint on the internal rotation of main-sequence stars. For low-mass solar metallicity stars we can use observations of subgiants (PKSD); however, the slow rotation of these stars is relatively difficult to measure. By contrast, there is detected (and in some cases, substantial) rotation on the horizontal-branch for metal-poor stars; solar metallicity stars of comparable mass have not yet reached this evolutionary phase (and won't do so for another 25 Gyr).

We begin by summarizing the available observations of main-sequence stars in § III*ai*. In § III*aii*, we convert the observed rotation velocities to lower limits on the total angular momentum on the horizontal branch, and analyze the data to look for dependencies on metallicity, age, and giant branch mass loss.

i) *Main-Sequence Surface Rotation Velocities*

It has been known for some time that metal-poor stars rotate slowly (for example, see Kraft 1967); determining just how slowly they rotate has proved more difficult (or perhaps, less interesting to observers?). Peterson, Tarbell, and Carney (1983) obtained an upper limit on the rotation velocity of 8 km s^{-1} for the main-sequence halo stars in their sample. With the exception of tidally locked binaries, which do not experience the same rotational history as other stars, we have not been able to find any direct detections of rotation in normal metal-poor stars, or more stringent upper limits, in the literature. This is not surprising, in light of their old ages and the observational evidence for angular momentum loss in low mass Population I stars. One nearby halo dwarf, Groombridge 1830 (= HD 103095) (Noyes *et al.* 1984; Noyes, Weiss, and Vaughan 1984), has a period estimate based on extrapolating the Noyes *et al.* 1984 relationship between the mean chromospheric activity level and the rotation period for solar metallicity stars to a halo star. We will discuss the potential implications of this interesting observation in § III*b*.

ii) *Total Angular Momenta on the Horizontal Branch*

The observations of rotation velocities on the horizontal branch could be directly compared with model rotation velocities if we had evolved models from the main sequence up the giant branch to the helium flash. We have evolved models only to main-sequence turnoff, so we cannot make such a direct comparison. However, we can compare the minimum total angular momentum inferred from surface rotation velocities on the horizontal branch with the angular momentum content in the interior of our main-sequence turnoff models. We begin with an overview of the rotation velocity observations, and then convert them into total angular momenta.

In Figure 1*a*, we present the detected rotation velocities and inferred total angular momenta (J_{tot}[HB]) as a function of T_{eff} for the complete Peterson (1983; 1985*a*, *b*) globular cluster sample. We have converted from $B-V$ to T_{eff} using the Yale color conversion program (Green *et al.* 1987, Green 1988) with reddening estimates from Harris and Racine (1979). The error

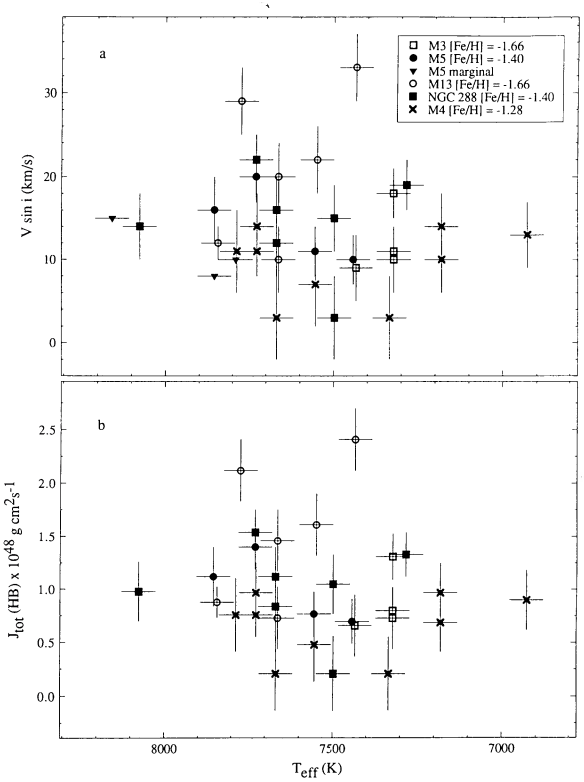

FIG. 1.—The observed rotation velocities (*panel a*) and inferred total angular momenta (*panel b*) of cluster horizontal-branch stars in the Peterson (1983, 1985*a*, *b*) sample as a function of effective temperature. Definite detection of rotational broadening was claimed for rotation velocities of 15 km s^{-1} or higher. The rotation velocities are in km s^{-1} and the angular momenta are in units of 10^{48} g cm^2 s^{-1}. The different symbols denote observations in different clusters; inferred angular momenta have not been computed for marginal detections of rotation in M5.

bars on the v sin i's are from Peterson; the errors of ± 50 K in $T_{\rm eff}$ were estimated from an assumed error in $B-V$ of 0.01.

The stars in M13 appear to have systematically higher rotational velocities than stars in other clusters, and the stars in M4 appear to have systematically lower rotation velocities. Other than this, Figure 1*a* does not show convincing differences in rotation velocities from cluster to cluster. In view of the large star-to-star variations within each cluster and the small sample, the systematic trend in mean cluster rotational velocities as a function of horizontal-branch morphology pointed out by Peterson (1985*a*, *b*) can at best be regarded as suggestive.

Within the uncertainties, Figure 1*a* does not show a convincing correlation between [Fe/H] and surface rotational velocity. The sample also includes two sets of clusters, each with nearly the same metallicity, that exhibit the "second parameter" effect of horizontal-branch morphology (LDZ): M3 and M13 ([Fe/H] = -1.66, Zinn and West 1984) and in a milder form M5 and NGC 288 ([Fe/H] = -1.40, Zinn and West 1984). There is a clear separation in Figure 1*a* between M3 and M13, but no significant difference between M5 and NGC 288. Since there are theoretical indications (DDP, § IIIciii) that $J_{\rm tot}$(HB) may depend on both turnoff mass and metallicity we emphasize the need for more precise observations of a larger sample of horizontal-branch stars to clarify this issue.

The lower limits on the total angular momentum on the horizontal branch, $J_{\rm tot}$(HB), were inferred from the surface rotation velocities as follows. Assuming rigid rotation on the horizontal branch, $J_{\rm tot}({\rm HB}) = I_{\rm tot}({\rm HB})v_{\rm surf}({\rm HB})/R({\rm HB})$, where $v_{\rm surf}$ is the surface rotation velocity, $I_{\rm tot}$ is the total moment of inertia, and R is the total stellar radius. The conservative assumption of rigid rotation is necessary in the absence of giant-branch models with rotation; it is also plausible for several reasons. In the absence of mean molecular weight gradients, the helium core on the giant branch would rotate rigidly or nearly so; it is also possible that the violent helium flash would reduce angular velocity gradients between the surface and the core.

In any case, rigidly rotating horizontal-branch models provide a reasonable *lower limit* to the angular momentum content on the horizontal branch. We have constructed standard horizontal-branch models similar to those of Lee and Demarque (1990) to determine $I_{\rm tot}$ and R as a function of color and metallicity, and have explored the variation of these quantities during horizontal-branch evolution.

The moment of inertia and radius of a horizontal-branch model depends on the metallicity, mass, and evolutionary state. Higher metallicity implies that a model of a given mass is redder. As a result, at fixed color a relatively metal-poor model is more massive than a relatively metal-rich model and has a larger moment of inertia. This effect must be included when comparing observations of clusters with different metallicities.

Horizontal-branch stars become redder as they evolve toward the asymptotic giant branch. This has two effects. At a fixed color, a given horizontal-branch star can have a range of possible masses. A given star could be either a relatively high mass unevolved star or a relatively low mass, but more evolved, star (LDZ). Because the moment of inertia increases as the models evolve, and because redder models tend to be more massive, the moment of inertia also increases as $T_{\rm eff}$ decreases.

The observed velocities are related to the inferred total angular momenta by the factor $I_{\rm tot}/R$. A range in mass of 0.08 $M_\odot$ gives a range in $I_{\rm tot}/R$ of 10%, while models with metallicity $Z = 4 \times 10^{-4}$ have $I_{\rm tot}/R$ systematically 5% larger than models of the same color with $Z = 10^{-3}$. Over the temperature range of the observations (7000–8000 K) $I_{\rm tot}/R$ is virtually independent of the effective temperature. We therefore conclude that a given surface rotation velocity can be reliably converted to a lower limit on the total angular momentum, with a relatively small range of $\pm 10\%$ primarily due to the uncertainty in the total mass at a fixed color.

How much angular momentum do metal-poor stars have on the horizontal branch? In Figure 1*b* we have converted the observations into lower limits on the total angular momentum content on the horizontal branch. There is a 10%–20% uncertainty in the rotation velocity estimates for the most rapid rotators, with higher relative uncertainties for the slow rotators. Combined with the uncertainties in converting a given rotation velocity to a total angular momentum, this indicates that the inferred total angular momenta are accurate to within $\pm 20\%$–30% for the rapid rotators.

In addition to the scatter caused by observational error and errors introduced in converting rotation velocities to angular momenta, there may be two other causes for the scatter in $J_{\rm tot}$(HB) in Figure 1*b*. One is the effect on v sin i of a random inclination of the rotation axis of the stars to the observer; the other is the possibility of an intrinsic distribution of $J_{\rm tot}$(HB). In view of the small sample and large relative uncertainty in the rotation velocities of the slow rotators there is insufficient data to infer a dispersion in total angular momentum. For the same reasons, average angular momenta are likely to understate the true total angular momentum on the horizontal branch. Because the largest rotation velocities are most accurately measured, and form a stronger constraint on the minimum $J_{\rm tot}$(HB), we will use the star with the maximum angular momentum inferred in each cluster to determine $J_{\rm tot}$(HB) for that cluster.

In all the clusters (except M4) there are total inferred angular momenta of at least 1.5×10^{48} g cm^2 s^{-1}, with a substantially larger value in M13. We therefore take $J_{\rm tot}({\rm HB}) \sim 1.5 \times 10^{48}$ g cm^2 s^{-1} and consider the degree of surface rotation on the main sequence required to retain this much angular momentum on the horizontal branch for our models (§ III*c*), and for rigidly rotating models with different treatments of post–main-sequence angular momentum loss (§ III*d*).

b) Surface Main-Sequence Rotation: Models Compared with Observations

We have two observational constraints on models of metal-poor stars: they must rotate slowly on the surface at turnoff and they must retain enough internal angular momentum to explain the observed horizontal-branch velocities. *The metal-poor models satisfy both observational requirements quite naturally.* They have slow surface rotation rates at main sequence turnoff, while their substantial differential rotation with depth allows them to preserve an adequate reservoir of internal angular momentum. Here we discuss the evolution of the surface rotation rate, and then turn (in § III*c*) to the evolution of the internal rotation curve.

Angular momentum loss acts to spin-down the surface layers of models to a fraction of their initial rotation rate. The surface rotation velocities of models with angular momentum loss from a magnetic wind all follow the same general pattern (see PKD for details in the solar metallicity context); we begin

by outlining the morphology of the spin-down of such models and then compare the metal-poor models to solar metallicity ones. The surface rotation velocity initially increases during the PMS phase as the model contracts while approaching the main sequence. As the surface angular velocity rises the degree of angular momentum loss increases dramatically; for our basic angular momentum loss law, $dJ/dt \sim \omega^3$ (Kawaler 1988). At some point (that depends on the mass, composition, and initial angular momentum) the surface rotation velocity starts to drop as the increase in the surface rotation rate from contraction is overcome by angular momentum loss. This decrease can be substantial in the pre-main sequence for rapid rotators, but is negligible until the main sequence for slow rotators.

Regardless, when the model arrives on the main-sequence contraction ceases and the magnetic wind acts to rapidly brake the surface convection zone. This generates a strong shear at the base of the surface convection zone, which triggers rotational instabilities. The instabilities then act to transport angular momentum from the interior to the surface; this angular momentum transport occurs in part through mass motions, i.e., mixing. Because the instabilities are inhibited by density and mean molecular weight gradients, the interior will not in general spin-down to the same angular velocity as the surface. The pattern of spin-down in the outer layers followed by angular momentum transport propagated through the interior will continue throughout the main-sequence evolution. As the rotation rate decays, however, the rate of angular momentum loss and internal angular momentum transport will decline.

The surface rotation periods of the halo star models are strikingly similar to those of Population I models with the same mass; by an age of a few $\times 10^8$ years, models with very different metallicity but otherwise identical parameters have similar surface rotation periods. To understand this result, it is convenient to divide the evolution of the surface rotation velocity into two phases.

The surface rotation velocity is initially sensitive to a variety of effects. The memory of the initial conditions has not yet been erased, and the interior has not yet had time to respond to the initial spin-down of the surface convection zone. The structure is also changing rapidly during the pre–main-sequence phase. Angular momentum loss, which is strongly dependent on the surface rotation rate, subsequently acts to remove differences in the surface rotation rate between models with different initial angular momenta; at the same time, instabilities begin to efficiently transport angular momentum from the interior to the surface.

Once the age of the models exceeds the time scale for operation of the instabilities, the interior can be regarded as coupled to the surface for angular momentum purposes (i.e., a change in the surface angular velocity is propagated throughout the interior). As discussed in PKD and PKSD, the model then settles into an asymptotic phase where the form of the angular momentum loss law, and the total moment of inertia determines the time dependence of the spin-down. Because the total moment of inertia on the main sequence is almost exclusively a function of mass, models with very different metallicity and the same mass will eventually settle down to nearly the same surface rotation period given the same angular momentum loss law.

The surface rotation velocities of our models are therefore primarily sensitive to the angular momentum loss law. Our angular momentum loss model has been calibrated on main-sequence Population I stars; how do our model compare with observations of metal-poor stars? Our models rotate at a rate that is well below the observed upper limit; for ages in excess of 10 Gyr the surface rotation velocities of the models are of order 1 km s^{-1} or less. (For details, see the tabulated rotation velocities and periods in PDD).

Furthermore, the inferred surface rotation velocities are very low for a wide range of angular momentum loss laws and time scales for internal angular momentum transport. A change in the wind index N (see PKSD for a definition) from 1.0 to 2.0 corresponds to a large change in the dependence of the angular momentum loss rate on the angular velocity ω; from $dJ/dt \sim \omega^{7/3}$ to $dJ/dt \sim \omega^{11/3}$. Even these drastically different angular momentum loss formulations cause changes in the surface rotation velocities of rapid rotators of only up to 0.09 km s^{-1}, or 12%, at an age of 10 Gyr (Table 1, § IIIciv). Varying the time scale of internal angular momentum transport by an order of magnitude up and down produces a change in the surface rotation velocities of only up to 0.23 km s^{-1}, or 45% (see § IIIciv for further discussion). The surface rotation of our models is therefore consistent with the observational upper limits for a wide range of solar calibrated cases. This indicates that the same physical assumptions used for solar metallicity models can be applied successfully to metal-poor models. At the same time, the surface main-sequence properties of metal-poor models cannot be used to distinguish between different possible angular momentum loss and transport histories with currently available data.

One star, HD 103095 (Noyes *et al.* 1984; Noyes, Weiss, and Vaughan 1984), has a period estimate based on extrapolating the Noyes *et al.* 1984 relationship between the mean chromospheric activity level and the rotation period for solar metallicity stars to a halo star. Based on an effective temperature of 5075 K and a metallicity [Fe/H] of -1.4, our models give a mass of order 0.6 $M_\odot$. The inferred period of 34.0 days corresponds to a $v \sim 0.8$ km s^{-1}, which is extremely slow in absolute terms but higher than the rate ($v \sim 0.22$–0.24 km s^{-1}, or a period of 113–124 days) our models would predict. *Because the degree of surface rotation is extremely small in any case, however, differences at this level would have a minimal effect on the global properties of the models at the main-sequence turnoff.* It is nonetheless interesting to consider the possible reasons for the higher than expected inferred rotation of HD 103095.

Because the period is estimated from the Noyes *et al.* 1984 empirical relationship for solar metallicity stars, there could be some systematic error in the period estimate introduced by the stars' low metallicity. The same relationship may not hold for halo stars; for this reason a direct period measurement for this star would be highly desirable. Such a measurement, in conjunction with other direct period measurements for halo stars, would also allow an empirical calibration of the relationship between chromospheric activity and rotation period for metal-poor stars. Because it is in general easier to measure the mean level of chromospheric activity than to directly measure rotation periods, this would allow a relatively large sample of rotation period estimates for metal-poor stars to be generated with a modest investment of observing time.

Alternately, if the higher than expected rotation in this star is confirmed, it may indicate that metal-poor stars have different angular momentum loss properties than solar metallicity stars. One possibility is that below some critical rotation rate the stellar dynamo loses coherence and further angular momentum loss ceases (Durney and Latour 1978). During their long

lifetime, metal-poor stars could thus have spun-down until their surface rotation was too low to support a dynamo; their surface rotation velocities would then be slightly higher than one would expect if angular momentum loss continued throughout their lifetime. Because solar cycle-like variations in activity have been observed in HD 103095, however, it is unlikely that this star is magnetically dead. There is also the implausible possibility that Groombridge 1830 might be a younger star: for $v = 0.8$ km s^{-1}, however, our corresponding model has an age of only 1 Gyr.

The halo stars may also have an angular momentum loss law with a different time dependence than the empirical Population I Skumanich (1972) $v \sim t^{-1/2}$ relation, or with a different constant term in the angular momentum loss law than that derived from the solar calibration. Differences of this sort would affect the history of the spin-down of such stars, and the timing of any mixing within them, but would have a minimal impact on their inferred global properties at turnoff.

Direct measurements of rotation periods of main-sequence, metal-poor stars will be required to resolve these issues. Better upper limits on $v \sin i$ at turnoff would also be extremely useful, especially for the comparison with evolved star rotation discussed in § IIIc. Accurate determination of halo star rotation velocities could also potentially be used as an age indicator for these stars, in the same fashion as for solar metallicity stars (PKD, Kawaler 1989). Because the expected rotation rates are slow, however, even small errors in the rate could lead to large uncertainties in age. Using rotation as an age indicator may therefore be a difficult task to implement in practice for halo stars.

c) *Internal Main-Sequence Rotation: Main-Sequence Models Compared with Horizontal-Branch Observations*

The rapid rotation of horizontal-branch stars, combined with the slow rotation of main sequence metal-poor stars, provides striking evidence for differential rotation with depth in stars. We cannot directly compare the horizontal branch rotation velocities with those of the models because we have not evolved our models past main-sequence turnoff. However, the angular momentum content of the core of a main-sequence turnoff model can be compared with the total angular momentum on the horizontal branch. In § IIIci we list and justify the assumptions that are required to make a comparison of the turnoff models and the horizontal-branch observations.

In § IIIcii we compare theory and observations for our basic set of rotation parameters. The angular momentum content of stars at the main-sequence turnoff, and the angular momentum transport properties of giant branch stars, also depend on the age, total stellar mass, and composition of the star. We thus analyze the angular momentum content of models as a function of turnoff mass (and therefore cluster age) and metallicity in § IIIciii and compare with observed properties as a function of age and metallicity. In § IIIciv we test the consequences of changes in the rotation parameters.

i) *Assumptions Used to Compare Main-Sequence Models with Horizontal-Branch Observations*

As models evolve from the main sequence to the giant branch, and up the giant branch, the surface convection zone deepens substantially. All but 0.3–0.4 $M_\odot$ of material is at some point part of the surface convection zone (i.e., the convection zone contains 0.4–0.5 $M_\odot$ at its maximum depth). Substantial mass loss ($\sim$0.15 $M_\odot$) on the giant branch is required to explain the difference between the turnoff and horizontal branch masses of globular cluster stars (§ I). Because there are sound observational and theoretical reasons why rigid rotation should be enforced in convective regions (§ IIIe), we will concentrate on models which assume rigid rotation in convection zones.

To a good approximation, the bulk of the angular momentum in the surface convection zone on the giant branch will be lost because of this giant branch mass loss. For a rigidly rotating surface convection zone, the material near the surface will have higher than average specific angular momentum because of its large moment of inertia. As the outer layers are lost, mass loss will thus carry away a large fraction of the angular momentum contained in the surface convection zone (§ IIIdii). If a magnetic wind is operating, then even more drastic angular momentum loss would ensue. Furthermore, this argument is almost independent of the mass-loss history on the giant branch (§ IIIdii).

It is therefore difficult to preserve a large reservoir of angular momentum in the outer layers of giants. However, if differential rotation in the radiative interior is allowed then the angular momentum in the core could survive all the way to the horizontal branch without being affected by giant branch mass loss. From the models, we have the angular momentum distribution at main sequence turnoff. In general, instability mechanisms will transport angular momentum from the radiative core to the convective envelope as the models ascend the giant branch. A direct comparison of the models with the observations will therefore require evolving the models up the giant branch.

By considering the case where there is no transport of angular momentum from the core to the convective envelope, however, we can already determine the *maximum* angular momentum the models could arrive with on the horizontal branch. Following the notation of DDP, we can define a critical mass fraction M_p(max), such that material with $M(r) \leq M_p$(max) is never part of the surface convection zone on the giant branch. M_p(max) is a moderately strong function of metallicity but only a weak one of total stellar mass. For turnoff masses between 0.725 $M_\odot$ and 0.8 $M_\odot$, M_p(max) ranges from 0.3134 to 0.3199 $M_\odot$ for $Z = 10^{-3}$ models and from 0.3686 to 0.3750 $M_\odot$ for $Z = 10^{-4}$ models. Define $J_{\rm core}$ as the angular momentum contained within $M(r) \leq M_p$(max). In the absence of angular momentum transport from the core to the envelope, our models could retain as much angular momentum as $J_{\rm core}$ even if all the angular momentum in the outer layers was lost; $J_{\rm core} \geq J_{\rm tot}$(HB) is therefore the condition our models must satisfy.

ii) *Properties of the Basic Case*

For a wide range of turnoff masses and metallicities, our models contain sufficient internal angular momentum to explain the horizontal branch observations. We begin by looking at models with high initial angular momentum (J_0). As we will see in § IIIciv, the angular momentum content depends only weakly on the value of J_0 until J_0 becomes small. We present the core and total angular momenta at main-sequence turnoff in Table 1. From Table 1, our models have 1.6–3 times as much core angular momentum as is required to explain the horizontal-branch observations. As we will see in § IIIdii approximately one-eighth of the envelope angular momentum survives the giant branch mass loss for a typical total giant branch mass loss of 0.15 $M_\odot$. In the absence of transport of angular momentum from the core to the envelope, therefore, the total angular

TABLE 1

COMPARISON OF MODELS (0.75 $M_\odot$, at 10 Gyr) WITH DIFFERENT ROTATIONAL PARAMETERS

N (1)	V_{ss} (2)	R_{crit} (3)	F_μ (4)	K_w (5)	F_c (6)	v_{surf} (km s^{-1}) (7)	Δv_{surf} (%) (8)	J_{tot} (10^{48}) (9)	ΔJ_{tot} (%) (10)	J_p (10^{48}) (11)	ΔJ_p (%) (12)
1.5.....	1.0	1000	1.0	2.46	0.034	0.71	...	5.61	...	3.01	...
2.0.....	1.0	1000	1.0	0.22	0.047	0.80	+12	5.22	−8	2.82	−6
1.0.....	1.0	1000	1.0	29.5	0.025	0.69	−3	6.08	+8	3.22	+7
1.5.....	0.1	1000	1.0	4.8	0.07	0.52	−28	9.44	+68	5.52	+83
1.5.....	10.0	1000	1.0	1.75	0.014	1.04	+45	3.62	−35	1.75	−42
1.5.....	1.0	15,000	1.0	4.9	0.05	0.86	+21	7.38	+32	3.65	+21
1.5.....	1.0	1000	0.1	2.46	0.034	0.82	+15	5.44	−3	2.37	−21
1.5.....	1.0	1000	10.0	2.46	0.034	0.58	−19	5.83	+4	3.58	+19

NOTE.—The rotational parameters for the different models are presented in columns (1)–(6) and their global properties are presented in columns (7)–(12). For definitions of the parameters, see text and PKSD. The first row is the canonical model with our default parameter values. The second and third rows have different angular momentum loss laws; the fourth and fifth have different time scales for angular momentum transport; and the sixth, seventh, and eighth rows have different stability conditions for the angular momentum transport mechanisms. Columns (7), (9), and (11) are the surface rotation velocity in km s^{-1}, the total angular momentum, and the core angular momentum (*see text for definition*) in units of 10^{48} g cm^2 s^{-1}, respectively. Columns (8), (10), and (12) are the percentage differences of these quantities from the canonical model.

momentum on the horizontal branch would range from 2.6–4.3 × 10^{48}, or 2–3.2 times as much as needed.

Do our models have too much internal angular momentum? In fact, it is extremely unlikely that no angular momentum is transported from the core to the envelope during the giant branch phase of evolution. Our comparison is therefore extremely conservative. By applying a consistent evolutionary treatment of angular momentum transport to both the main sequence and the giant branch, the requirement that the models retain *as much as* 1.5 × 10^{48} in angular momentum by the horizontal branch will place stringent constraints on the ability of angular momentum redistribution to overcome mean molecular weight and density gradients. The presence of differential rotation with depth on the horizontal branch would increase the inferred horizontal branch angular momenta and place even more severe restrictions on internal angular momentum transport.

How do our results compare with the solar metallicity models? The differences in internal rotation between the halo star and Population I star models are as striking as the similarities in their surface rotation. Like more massive Population I stars, the thin surface convection zones of the halo star models spin down quickly and it takes tens to hundreds of millions of years for the interior to respond. Unlike the more massive Population I stars, strong differential rotation with depth is tolerated by the structure of metal-poor models. A good rule of thumb is that the vigor of angular momentum redistribution mechanisms decreases with decreasing mass. In addition, the shear instability, which dominates angular momentum redistribution near the base of the surface convection zone, tolerates more and more differential rotation with depth as the mass decreases.

In Population I stars, rigid rotation is enforced in the deep surface convection zones of low-mass stars and this structural feature reduces differential rotation with depth. The thin surface convection zones of halo stars, on the other hand, allow differential rotation with depth to begin much further out in the star and to reach a greater contrast between central and surface rotation. For the same surface rotation rate and mass, therefore, halo models retain more of their internal angular momentum than Population I models do.

iii) *Effects of Changes in Metallicity and Turnoff Mass*

The total angular momentum at main sequence turnoff is a function of both mass (and thus turnoff age) and metallicity. A change in total mass from 0.725–0.800 $M_\odot$ or a change in metallicity from $Z = 10^{-3}$ to $Z = 10^{-4}$ both produce changes in the core angular momentum ~25%, with lower metallicity and higher mass models having higher core angular momenta. Given that we have not evolved these models up the giant branch, we cannot be certain that these trends will persist in the horizontal-branch observations. Furthermore, given the quality and quantity of the current data the magnitude of any observed cluster-to-cluster variations is difficult to assess, although some real variations do appear to be present (§ III*aii*). However, with a larger sample of horizontal-branch rotation velocities we will have the possibility of detecting systematic differences between clusters with different ages and of testing the metallicity dependence of differential rotation with depth in stars.

iv) *Effects of Changes in Model Parameters*

In this section we investigate the sensitivity of our results to changes in the rotational parameters. *Our models have substantial differential rotation with depth and low-surface rotation velocities for a remarkably wide range of rotational parameters.* These parameters fall into three categories: the time scale of angular momentum loss, the time scale of angular momentum transport, and the stability conditions for the transport mechanisms. For more detailed definitions and discussion, see PKSD.

The angular momentum loss rate is proportional to a constant (K_w) multiplied by the surface angular velocity raised to some exponent. The exponent determines the time-dependence of the spin-down. We can vary this exponent by changing the wind index N; our canonical case has $N = 1.5$, which corresponds to $dJ/dt \sim \omega^3$. This value reproduces the empirical Skumanich (1972) spin-down of open cluster stars (Kawaler 1988; PKSD). The constant is calibrated to reproduce the solar rotation rate at the age of the Sun for any given set of rotational parameters.

The secular shear instability (Zahn 1974) dominates angular momentum transport in the outer layers. To reflect uncer-

tainties in its time scale, we multiply the diffusion velocity estimate for the shear by a factor V_{ss} that is set to unity in our canonical case. The shear sets in whenever a critical Reynolds number (R_{crit}) is exceeded; the exact value determined in laboratory experiments ranges from 1000 to 15,000 depending on the geometry. We have chosen $R_{crit} = 1000$ for our canonical case, in line with Couette flow experiments (see Law 1980 for a discussion). As R_{crit} increases, the degree of differential rotation tolerated by the shear increases.

Finally, meridional circulation and the GSF instability are inhibited by mean molecular weight gradients; we estimate this effect by computing a fictitious "μ velocity" that acts to oppose transport. The μ velocity is multiplied by a factor F_μ that is set to unity in our basic case.

We now show how varying each of the parameters affects the surface velocity, total angular momentum, and core angular momentum of our halo models. For the purposes of this section, we shall refer to the combination of parameters ($Y = 0.24$, $\alpha = 1.4$, $M = 0.75\ M_\odot$, $Z = 0.0001$) as describing the "canonical" model sequence. Because the effects of varying the parameters are most noticeable for rapid rotators, we have looked at models with a high initial angular momentum ($\log J_0 = 50.2$).

For all alternate combinations of parameters discussed in this section, the T_{eff} at 10 Gyr falls within 1 K (!) of that of our canonical model sequence; this underscores the fact that rotation causes only a minor perturbation on the structure of standard halo models (DDP).

In all cases, the surface velocity, the total angular momentum, and the core angular momentum are within 45%, 68%, and 83%, respectively, of the canonical model's (Table 1). This consistency is remarkable in view of the fact that the canonical sequence has lost all but $\sim 1/30$ of the initial angular momentum, and rotates very slowly at the surface. Apparently, large uncertainties in the rotational parameters propagate into only small absolute differences in the final configuration: a sharp differential rotation curve is obtained for all sets of parameters. We now discuss each parameter separately.

We first address the possibility that the angular momentum loss law for Population II stars might be different than that for Population I stars. We find that model sequences with different N are nearly identical to the canonical sequence. For the extreme case of an efficient early spindown ($N = 2$, which represents a radial magnetic field), the sequence has lost slightly more angular momentum and ends up spinning faster at the surface, whereas for $N = 1$, the sequence retains slightly more angular momentum and spins more slowly at the surface. Note that a value of N near 1.5 is required to explain the observed spin-down of low-mass Population I dwarfs.

Varying the diffusion velocity estimate for angular momentum transport by the secular shear up and down by an order of magnitude gives the largest deviations from the canonical sequence. Lower velocities results in more angular momentum being retained by the models, especially in the deep interior, because less transport can occur in the early main sequence when mean molecular weight gradients are small; the opposite holds for a higher velocity estimate.

An increase in the critical Reynolds number to 15,000 implies the shear tolerates more differential rotation with depth. More angular momentum is therefore retained in the interior. Finally, varying the sensitivity of angular momentum transport to mean molecular weight gradients up and down by an order of magnitude affects primarily the core angular momentum: weaker inhibition by μ gradients results in less angular momentum being retained by the models, and vice versa.

To summarize: given the slow surface rotation of all the sequences, the absolute differences in the predicted surface rotation of main-sequence halo stars are probably too small to serve as a useful constraint on the rotational parameters. However, the changes in the internal rotation profile discussed above may be testable in evolved stars, particularly in the angular momentum content on the horizontal branch. We note that the differences in the core angular momentum content at main sequence turnoff will be accentuated to some degree by evolution on the giant branch. In fact, requiring consistency between horizontal-branch observations and giant branch models with rotation could provide the most sensitive constraint on the angular momentum content in the cores of stars. We nonetheless stress that the global properties of the models, namely rapid core rotation coupled with slow surface rotation, are present in all the cases considered here.

d) Models with Rigid Rotation Compared with Horizontal-Branch Observations

In this section we compare rigidly rotating models to the observations. Evolved horizontal branch stars are observed to rotate rapidly, while their main-sequence progenitors rotate slowly. Differential rotation with depth is the natural explanation for this combination of observations; these seemingly paradoxical constraints can be naturally reproduced by our models, which rotate differentially (§ III*c*). However, some theorists have argued that magnetic fields should enforce rigid rotation in stellar interiors over a short time scale.

The argument for rigid rotation in stellar interiors can be stated as follows. Differential rotation with depth in the radiative interiors of stars would amplify even a small internal magnetic field over a short time scale, generating toroidal magnetic fields strong enough to remove the angular velocity gradients (e.g., Spruit 1987; Mestel, Moss, and Tayler 1988). This hypothesis has been challenged by other theorists (e.g., Fox and Bernstein 1987; Tassoul and Tassoul 1989). Because of the severe theoretical uncertainties, and the almost total lack of observational constraints, we have not included angular momentum transport by magnetic fields in our models. Nevertheless, rigid rotation enforced on a short time scale makes unambiguous predictions about the rotation of stars as a function of time and evolutionary state that can be tested observationally.

The hypothesis of rigid rotation enforced on a short time scale runs into severe difficulty in explaining the observed rotation of white dwarfs and solar metallicity subgiants (PKSD) and the spin-down of young open cluster stars (Stauffer and Hartmann 1986; PKD). As we will show, the combination of slow main sequence rotation and rapid horizontal-branch rotation in metal-poor stars poses an even greater challenge for rigid rotation. Can rigid rotation enforced on a short time scale be reconciled with the observations?

We look at a series of different cases for post–main-sequence angular momentum loss, and at rigid rotation enforced over different time scales. For each case we determine the surface rotation velocities main-sequence turnoff stars would need to have to produce the observed horizontal-branch rotation velocities, given the assumed physics. § III*di* we look at models without post–main-sequence angular momentum loss. In § III*dii* we examine the behavior of more realistic rigidly rotat-

ing giant branch models with different giant branch mass loss histories. *Uniform rigid rotation on the giant branch is found to be ruled out by the observations once the effects of mass loss on the giant branch are taken into account.*

One may then ask whether or not it is still possible for rigid rotation in radiative regions to be enforced only on the main sequence. In § III*diii* we treat the case of rigid rotation enforced throughout the model on the main sequence, followed by local conservation of angular momentum in the radiative interior and rigid rotation in the surface convection zone. *Rigid rotation in the interior is then found to be incompatible with the observations even if it is enforced only on the main sequence.* A summary of the inferred main-sequence rotation for the different cases with the main-sequence observations is presented in § III*div*.

Differential rotation in convective regions would materially affect the degree of angular momentum loss on the giant branch. However, even the combination of rigid rotation in the radiative interior with the most extreme rotation law in convective regions is found to lead only to marginal agreement with the current main-sequence limits; differential rotation with depth in convective regions causes other observational problems as well (§ III*e*). In any case, from the rotation of subgiants, differential rotation with depth in convective regions would require differential rotation with depth in the radiative interiors of their main-sequence progenitors (§ III*e*).

i) *No Post-Main Sequence Angular Momentum Loss*

When comparing rigidly rotating main-sequence models with the HB observations and the MS upper limits, the approach that is most favorable for rigidly rotating models is to assume that all of the main-sequence angular momentum somehow survives intact all the way to the horizontal-branch phase even though the outer layers have been lost. If rigid main-sequence rotation cannot explain the observations with this generous approach, then it will certainly fail once the important post–main-sequence effects are included.

In the absence of post–main-sequence angular momentum loss it is straightforward to compare rigidly rotating models with the observations. For rigid rotation, $J_{\rm tot} = v(I_{\rm tot}/R)$, where $J_{\rm tot}$ is the total angular momentum, v is the surface rotation velocity, $I_{\rm tot}$ is the total moment of inertia, and R is the stellar radius. Because $I_{\rm tot}/R$ increases from the main-sequence turnoff to the tip of the giant branch, for fixed $J_{\rm tot}$ the rotation velocity will be a maximum at main-sequence turnoff. A comparison of turnoff models with the MS upper limits therefore provides the best constraint on rigid rotation prior to the helium flash. For turnoff ages ranging from 12–20 Gyr, the turnoff masses range from 0.725 to 0.825 $M_\odot$. For this range of masses, the quantity $I_{\rm tot}/R$ at turnoff varies from 4.926–5.235 $\times$ 10^{42} (in cgs units) for $Z = 10^{-3}$ and from 4.349–4.726 $\times$ 10^{42} for $Z = 10^{-4}$. We can define a surface rotation velocity at main-sequence turnoff such that the rigidly rotating models have $J_{\rm tot}({\rm MS}) = J_{\rm tot}({\rm HB})$ by using the $I_{\rm tot}/R$ values defined above. For masses from 0.725 to 0.825 $M_\odot$, this critical velocity ranges from 3.0 to 2.85 km s^{-1} for $Z = 10^{-3}$ and from 3.45 to 3.15 km s^{-1} for $Z = 10^{-4}$. The most rapidly rotating field stars and stars in M13 would require velocities approximately one-third higher, or $\sim$4 km s^{-1}. This is rapid compared with younger Population I stars, but below the current limits (§ III*di*).

ii) *Rigidly Rotating Models With Steady Giant Branch Mass Loss*

Giant branch mass loss will drastically decrease the angular momentum content of rigidly rotating models. For rigid rotation, the angular momentum is highly concentrated in the outer layers because the bulk of the moment of inertia resides there. The material at the surface will therefore have higher specific angular momentum than the average for the entire star. Mass loss at the surface will therefore drain angular momentum from the star even in the absence of a magnetic wind.

The substantial inferred total mass loss (of order 0.15 $M_\odot$) between turnoff and the horizontal branch could either be a sudden ejection of mass at the helium flash, or a steady giant-branch process, or some combination of both. As we will see, the fraction of the angular momentum lost is a relatively weak function of the mass loss history on the giant branch. If mass loss is a steady giant-branch process, we can estimate the associated angular momentum loss as follows. For the mass loss rate ($\dot{M}$) at a given point on the giant branch, we use the empirical Reimers (1975) relation,

$$\dot{M} = K \frac{L}{gR} . \tag{1}$$

In this equation L is the total luminosity, g is the surface gravity, and R is the radius. The constant K is adjusted to give the desired total mass loss, integrated over the entire giant branch evolution. The associated angular momentum loss ($\dot{J}$) is equal to the mass of the ejected material multiplied by its angular velocity and moment of inertia, or

$$\dot{J} = \tfrac{2}{3}\dot{M}\omega R_{\rm surf}^2 , \tag{2}$$

where ω is the angular velocity and $R_{\rm surf}$ is the total stellar radius. For a rigid rotator the total angular momentum $J_{\rm tot} = \omega I_{\rm tot}$, where $I_{\rm tot}$ is the total moment of inertia. The fractional angular momentum loss in a given time step is therefore

$$\frac{\Delta J}{J_{\rm tot}} = \frac{2}{3}\frac{\Delta M R_{\rm surf}^2}{I_{\rm tot}} , \tag{3}$$

where ΔM is the total mass loss during the time step. The fraction of the initial angular momentum retained at the end of a given time step is equal to $1 - \Delta J/J_{\rm tot}$. The fraction of the angular momentum retained at the helium flash is equal to the product of the individual quantities $(1 - \Delta J/J_{\rm tot})$ over the entire giant branch evolution.

We evolved a standard giant branch sequence with $Z = 10^{-3}$ and $M = 0.8\ M_\odot$ to the helium flash. For each time step we evaluated the mass loss and the fractional angular momentum loss. We considered cases with the constant in the mass-loss rate adjusted to give total giant-branch, mass-loss rates ranging from 0.05–0.30 $M_\odot$. The change in surface gravity from the mass loss was taken into account when computing the mass-loss rate, but the total radius was assumed to be unaffected by the mass loss. (This is a reasonable approximation because the total radius of a giant branch model is only weakly dependent on the total mass).

For our estimate of the giant branch angular momentum loss rate, we have assumed that mass loss had no effect on the total moment of inertia. Because mass loss will lower the total moment of inertia, this conservative assumption underestimates the true angular momentum loss rate and thus the minimum surface rotation velocity on the main sequence. If one-half of the envelope mass is lost, the moment of inertia will drop by approximately a factor of 2 as well; the true fraction of angular momentum retained could therefore be substantially less than in the present calculations.

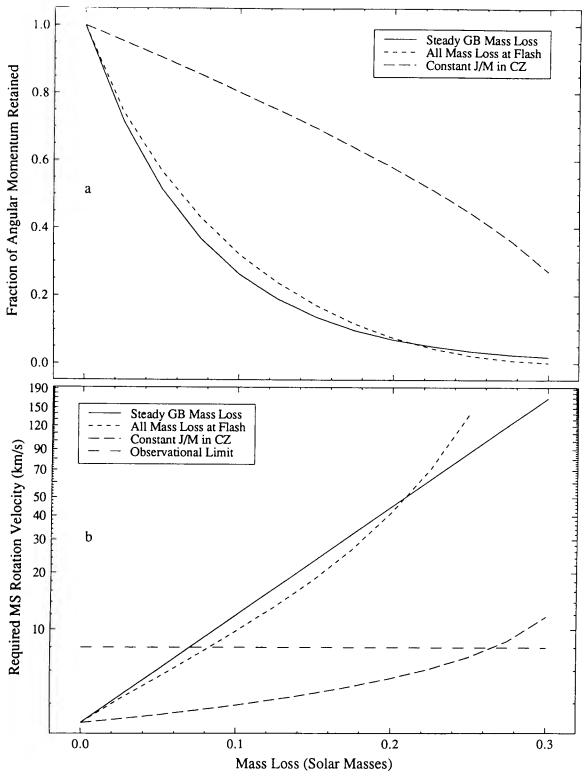

FIG. 2.—The fraction of the main-sequence turnoff angular momentum retained as a function of total giant branch mass loss (in solar masses) is presented in panel (*a*) for three cases: (1) rigid rotation in the surface convection zone and steady giant branch mass loss from a Reimers (1975) loss rate; (2) as case (1) except with all mass loss at the helium flash; and (3) as case (1) except with constant specific angular momentum in the surface convection zone. In panel (*b*) we show (as a function of the total giant branch mass loss) the main sequence surface rotation velocity a rigid rotator would need to retain enough angular momentum on the horizontal branch to explain the observations. The observational limit on the main-sequence rotation velocities is denoted by the horizontal line. For a typical total giant branch mass loss of 0.15 solar masses cases (1) and (2) are well above the observed limit; a range in mass-loss rates would also produce a strong dependence of rotation velocity on effective temperature that is not seen.

The fractional angular momentum loss as a function of the total giant branch mass loss is illustrated in Figure 2*a*; in Figure 2*b* we also show the inferred main-sequence rotation velocities required to preserve a total angular momentum on the horizontal branch of 1.5×10^{48}. From Figure 2, the fraction of the initial angular momentum that survives drops by approximately one-half for every 0.05 $M_\odot$ of mass loss on the giant branch; a typical mass loss scenario of 0.15 $M_\odot$ would imply extremely rapid surface rotation velocities at main-sequence turnoff of 24 km s^{-1}, in sharp contradiction with the data. As before, the most rapidly rotating stars in M13 would require velocities approximately one-third higher (or $\sim$32 km s^{-1}).

On average, horizontal branch stars with different color have experienced different degrees of mass loss. *If the bulk of the horizontal branch angular momentum came from the envelope then the observed horizontal-branch rotation velocities should be a strong function of the total mass loss, and thus horizontal-branch color.* There is no observational evidence for such a trend, which is another serious problem for rigidly rotating models.

Uniform rigid rotation therefore has serious problems with the combination of slow main sequence and rapid horizontal branch rotation for steady giant branch mass loss. However, what if all the mass is lost during the helium flash instead? For a rigid rotator, the fraction of the angular momentum lost is then equal to the fraction of the total moment of inertia lost. The fractional angular momentum loss as a function of the total mass loss, and the inferred main sequence rotation velocities required to preserve $J_{\rm tot}({\rm HB}) = 1.5 \times 10^{48}$ is compared to the case of steady giant branch mass loss in Figure 2. The fraction of the angular momentum lost is a relatively weak function of the mass-loss history, but a strong function of the total amount of mass loss for both cases. For mass loss of 0.15 $M_\odot$ at the helium flash excessively high surface rotation velocities of order 24 km s^{-1} are required at main-sequence turnoff, similar to the case of steady giant branch mass loss above.

iii) *Rigid Rotation Enforced to Main-Sequence Turnoff*

From the results of § III*d*ii, reconciling rigid rotation on the giant branch with the horizontal-branch observations would require rapid main sequence rotation, in contradiction to the observations (§ III*d*iv). Rigid rotation enforced on a time scale short compared to the post–main-sequence lifetime of metal-poor stars is therefore ruled out by the observations. However, what if the time scale for enforcing rigid rotation is shorter than the main-sequence lifetime ($\sim$15 Gyr) but longer than the lifetime of the subgiant and giant branch phases of evolution ($\sim$1.5 Gyr)? We can constrain such models as follows.

We have enforced rigid rotation until main-sequence turnoff; subsequently we have assumed local conservation of angular momentum in the radiative interior. Furthermore, we have assumed that all the material that was never part of the surface convection zone on the giant branch retains all of its main-sequence angular momentum, and that the convective envelope retains the same fraction of its main sequence angular momentum that was found in § III*d*ii above.

We can estimate the core and envelope angular momentum that survives until the horizontal branch as follows. Following the notation of DDP, let M_p be the mass (in solar masses) contained in the radiative interior when the surface convection zone reaches its maximum depth (in mass). Define $I_{\rm core}({\rm MS})$ as the moment of inertia for $M(r)/M_\odot \leq M_p$ and $I_{\rm env}({\rm MS})$ as the moment of inertia for $M(r)/M_\odot > M_p$. If rigid rotation is enforced on the main sequence, the angular momentum in the core $J_{\rm core}({\rm MS}) = \omega_{\rm surf} \times I_{\rm core}({\rm MS})$ and the angular momentum in the envelope $J_{\rm env}({\rm MS}) = \omega_{\rm surf} \times I_{\rm env}({\rm MS})$. For rigid rotation in convective regions, we can use the results of § III*d*ii to estimate the fraction f_J of the envelope angular momentum that survives the giant branch mass loss. For a total mass loss of 0.15 $M_\odot$, this fraction turns out to be $f_J \sim 0.128$.

$J_{\rm core}({\rm MS}) + f_J \times J_{\rm env}({\rm MS}) \geq J_{\rm tot}({\rm HB})$ must therefore be satisfied for the models to be consistent with the observed horizontal-branch rotation velocities. (Note that if f_J is set to 1, we recover the results of § III*d*i). We can therefore define a critical surface rotation velocity such that the main-sequence angular momentum equals the horizontal-branch angular momentum,

$$v_{\rm crit} = R \frac{J_{\rm tot}({\rm HB})}{I_{\rm core}({\rm MS}) + f_J I_{\rm env}({\rm MS})}, \quad (4)$$

where R is the total radius of the model at main-sequence turnoff.

For models with $Z = 10^{-4}$, we find $M_p \sim 0.37\ M_\odot$ and v_{crit} ranges from 16.8–17.1 km s^{-1} at main-sequence turnoff for masses from 0.725–0.80 $M_\odot$; for the same range of masses with $Z = 10^{-3}$, $M_p \sim 0.315\ M_\odot$ and v_{crit} ranges from 16.2–16.7 km s^{-1} at main-sequence turnoff. These large values are a consequence of the fact that the moment of inertia of the core is small; the ratio of the total moment of inertia I_{tot} to I_{core} for $Z = 10^{-4}$ ranges from 11.4–14.1 at main-sequence turnoff for masses from 0.725–0.80 $M_\odot$; for the same range of masses with $Z = 10^{-3}$, I_{tot}/I_{core} ranges from 14.9–18.5 at main-sequence turnoff.

A rigidly rotating main-sequence model therefore has little angular momentum stored in the core, and shielding this small reservoir from angular momentum loss on the giant branch has a relatively small effect on the main-sequence rotation velocity needed to explain the horizontal-branch rotation velocities. Once again the inferred main-sequence rotation velocities are well above the observed upper limits.

iv) *Rigidly Rotating Models Compared with Main-Sequence Rotation*

Rapid rotation on the horizontal branch severely constrains models with rigid rotation enforced throughout, even if the rigid rotation is enforced over a long time scale. In the preceeding subsections we have considered the surface rotation velocities at main-sequence turnoff required for the following cases: (1) No post–main-sequence angular momentum loss; (2) Rigid rotation enforced on a short time scale and angular momentum loss caused by different giant branch mass loss scenarios; and (3) Rigid rotation enforced on the main sequence only, with angular momentum removed from the surface convection zone on the giant branch in the same fashion as case 2.

The required rotation velocities range from ~ 3 km s^{-1} for case 1 to ~ 24 km s^{-1} for case 2 and ~ 17 km s^{-1} for case 3. The current observational upper limit on main-sequence rotation velocities is 8 km s^{-1} (Peterson, Tarbell, and Latham 1983). If convection zones rotate rigidly, therefore, angular momentum loss caused by giant branch mass loss rules out rigid rotation in the radiative interior, even if it is enforced only on the main sequence.

Furthermore, even the most extreme rotation law in convective regions (constant specific angular momentum) would allow rigid rotation in the radiative core only if surface rotation velocities at main-sequence turnoff were much higher than younger Population I stars (§ III*e*). Even if main-sequence stars were found to rotate at this rate, rigid rotation would still face a severe problem: stars with different degrees of giant branch mass loss would retain very different total angular momenta. The surface rotation velocity on the horizontal branch would then be a strong function of color; there is no observational evidence for such a trend.

Even the current low upper limit on main-sequence rotation velocities may be much higher than the true rotation rates of these stars. Current technology in high-resolution spectroscopy of main-sequence halo stars should be capable of detecting rotational broadening down to a much lower level, of order 2 km s^{-1} or less (Soderblom 1990). If the upper limits turn out to be as low as this (as the Noyes *et al.* 1984 period estimate for Groombridge 1830 suggests they might be), horizontal-branch stars would have more angular momentum than their main-sequence precursors if the latter rotate rigidly. This situation would be, at minimum, aesthetically displeasing. Post-main sequence mass loss would only accentuate the discrepancy. The rotation properties of metal-poor stars therefore constitute a strong counterexample to the hypothesis of rigid rotation enforced in the radiative interiors of stars.

Within the framework of our assumptions, the observed horizontal-branch rotation velocities place severe constraints on the ability of any angular momentum redistribution mechanisms to enforce rigid rotation in stars on even long time scales (comparable to the main-sequence lifetime of a metal-poor model, or $\sim 1.5 \times 10^{10}$ years). In light of the importance of this result, we analyze the validity of the steps that were taken to obtain it.

1. The inferred total angular momentum on the horizontal branch. We assumed rigid rotation on the horizontal branch when determining the angular momentum content there. If anything, we have underestimated this total angular momentum content because the structural evolution of giants produces strong differential rotation with depth which may not be entirely removed during the helium flash.

2. Angular momentum loss caused by giant branch mass loss. If convective regions rotate rigidly, there is no escape from the conclusion that the bulk of the angular momentum in the surface convection zone is lost because of giant branch mass loss. Our results are only weakly dependent on the turnoff mass used and the timing of the mass loss on the giant branch.

3. Internal angular momentum transport on the giant branch. For the case of rigid rotation enforced only until main-sequence turnoff, we considered the most extreme case, namely no transfer of angular momentum from the core to the convection zone during giant branch evolution. Given the strong differential rotation with depth generated by the structural evolution of giants, this is unlikely to be true. Taking such angular momentum transport into account would further increase the implied main-sequence rotation velocities (which are already too high).

Differential rotation with depth is therefore required to explain the rotational properties of metal-poor stars. However, could rigid rotation in the radiative interior still be enforced if differential rotation was present in the convection zone? We consider such models in the next section.

e) Consequences of Differential Rotation with Depth in Convective Regions

As we will show below, even very strong differential rotation with depth in convection zones is only marginally consistent with the observations when rigid rotation is enforced in radiative interiors. Strong differential rotation with depth in convective regions, however, presents a number of other observational difficulties. Estimates of the rotation of the solar convection zone inferred from inversion of *helioseismology* data (Libbrecht 1989) suggest that the solar convection zone rotates nearly rigidly; such inversions are most reliable in the outer layers of the Sun where the sensitivity of the inversion to differential rotation with depth is least uncertain.

Differential rotation with depth in convection zones also causes problems with the timing and mass-dependence of *lithium depletion* in Population I stars. Pre–main-sequence models have deep surface convection zones; these convection zones retreat to the surface as the models approach the main sequence. If convection zones tolerate substantial differential rotation with depth, models of all masses would arrive on the main sequence with enormous angular velocity gradients in the radiative interior. These gradients would be highly unstable and would cause an early phase of rapid mixing and angular momentum transport as the models readjusted to a more

stable angular momentum distribution. This mixing would cause both a sharp rise in the surface rotation velocities as angular momentum was transported from the core to the surface and dramatic early lithium depletion, in contradiction with observations.

Finally, the combination of rigid rotation in radiative regions and differential rotation in convective regions directly contradicts observations of *evolved Population I stars.* The angular momentum content of subgiants and giants is a minimum if their deep surface convection zones rotate rigidly; if there is substantial differential rotation with depth, then the implied angular momentum content is dramatically increased. When projected back to the main sequence, such large angular momenta could not be reconciled with rigid rotation at the observed surface rotation velocities (Pinsonneault and Sofia 1990). *Differential rotation with depth in convective regions therefore requires differential rotation with depth in the radiative interiors of massive stars.*

It is nonetheless interesting to consider the degree of differential rotation in the radiative interior that would be required in halo stars if convection zones do not rotate rigidly. Consider the most extreme case possible, namely constant specific angular momentum in convective regions. In this case, we can repeat the calculations of § III*d*ii and § III*d*iii with a simple expression for giant branch angular momentum loss: the fraction of the angular momentum in the surface convection zone lost in a timestep on the giant branch is equal to the fraction of the mass in the envelope lost, or

$$\frac{\dot{J}}{J_{\rm tot}} = \frac{\dot{M}}{M(\text{envelope})} . \quad (5)$$

For this purpose we define the envelope mass as the total mass outside the helium core. If the radiative interior rotates rigidly at the rate of the base of the surface convection zone, it contains only a small fraction (less than 1%) of the total angular momentum. The angular momentum loss from the surface convection zone for our sample $Z = 10^{-3}$, $M = 0.8$ $M_{\odot}$ model for steady giant branch mass loss was shown in Figure 2.

Angular momentum loss for a differentially rotating surface convection zone is clearly smaller than for a rigidly rotating one. However, a substantial fraction of the angular momentum is still lost. For a typical total mass loss of 0.15 $M_{\odot}$, ~70% of the angular momentum in the envelope is retained for the most extreme rotation law in convective regions. To retain $J_{\rm tot} \sim 1.5 \times 10^{48}$ at the tip of the giant branch, the star must therefore have left the main sequence with $J_{\rm tot} \sim 2.2 \times 10^{48}$. The surface convection zones of metal-poor models near main-sequence turnoff are extremely thin; if radiative regions rotate rigidly then the entire model essentially rotates rigidly. This would then imply a surface rotation velocity of 4 km s^{-1}, which is in accord with the current observational upper limit.

A better test of the rotation law in convective regions, however, is the rotation on the horizontal branch as a function of $T_{\rm eff}$. Horizontal-branch stars with different total masses in the same cluster (or clusters with comparable metallicity and age) have experienced different degrees of mass loss on the giant branch (LDZ). If convection zones rotate rigidly, then most of the angular momentum in the surface convection zone is lost and $J_{\rm tot}$(HB) should be weakly dependent (if at all) on the total mass.

If convection zones have constant specific angular momentum, on the other hand, the degree of angular momentum loss will be a strong function of the degree of mass loss. The observed surface rotation velocities on the horizontal branch would then be a strong function of $T_{\rm eff}$; from Figure 1, there is no evidence for such a trend. A larger sample of observations of horizontal branch rotation velocities as a function of color therefore provides the interesting potential to place even tighter constraints on the rotation law in convective regions.

IV. SUMMARY

From either the theoretical or observational viewpoint, the internal angular momentum distribution in stars has proven to be one of the most difficult stellar properties to determine. When trying to gauge the importance of rotation in stellar evolution it is also one of the most important. The rotational properties of metal-poor stars provide unambiguous evidence for differential rotation with depth in stars, and thereby provide strong constraints on models of internal angular momentum transport. Evolved solar metallicity stars also show evidence for differential rotation with depth. Rigid rotation enforced on a short time scale in low mass stars (by the action of internal magnetic fields, for example) has often been viewed as a simple and appealing assumption; it is also a powerful hypothesis that makes definite, and as we have demonstrated, testable, predictions about the rotation of evolved stars. *Because the observations contradict this hypothesis, a more complex model is needed.*

Observations indicate that internal magnetic fields do not enforce rigid rotation on a short time scale in these stars; it does not follow, however, they they are unimportant or must be absent. In the Sun and open cluster stars there is evidence that angular momentum transport is more effective than material mixing; magnetic fields provide an attractive mechanism for transporting angular momentum without mixing. *Angular momentum transport by the action of internal magnetic fields only runs afoul of observations when it is required that it be extremely effective over a short time scale.* These observations must therefore be taken as an indication that more theoretical work is needed, particularly in understanding nonlinear effects and the interaction of magnetic fields with turbulence and circulation currents induced by rotation.

Models with angular momentum loss from a magnetic wind and angular momentum transport from rotational instabilities can reproduce the general rotational properties of metal-poor stars. Furthermore, the observations of metal-poor stars can be reproduced with the same physical model as that used for solar metallicity stars. Rotationally induced mixing can also explain the surface light element abundances of main-sequence stars with a variety of ages, masses, and metallicities (PKD, PDD). Matching global constraints does not, of course, imply that the assumptions we have made in our models are accurate in all respects. Given the richness of physical systems, even the best models must incorporate simplifying assumptions that are at some level incorrect. However, consistent modeling of stars of a variety of ages, masses, and metallicities is the best way to test the general validity of our approach. Perhaps the most appealing feature of the rotational models is the way in which the global properties of a range of stars follow naturally from the same physical model.

Further refinements in theory, and more numerous and precise observations, will be needed to quantify the results obtained thus far. The low observed surface rotation velocities of metal-poor, main-sequence stars can be reproduced with angular momentum loss and transport properties appropriate

for solar metallicity stars. Because they are old and rotate slowly, however, main-sequence, metal-poor stars do not provide constraints on the time scales of angular momentum loss and transport as sensitive as those required to explain the rotational properties of solar metallicity open cluster stars. More stringent limits, or better yet detections, of rotation in main-sequence, metal-poor stars would enable us to place better constraints on both the main-sequence rotational properties and the degree of differential rotation with depth required to explain the observations. Observations of stars in clusters would be particularly informative.

A larger sample of high-quality, horizontal-branch rotation velocities would enable us to answer a series of questions. Does the angular momentum on the horizontal branch depend on metallicity or turnoff age? If so, such dependencies could be used to constrain the properties of the models.

Is there an intrinsic dispersion in total angular momentum at a given color, and does the total horizontal branch angular momentum depend on the color (and thus the degree of giant branch mass loss)? The amount of envelope angular momentum that survives giant branch mass loss depends on the total mass loss, while the amount of core angular momentum retained will depend weakly (if at all) on the mass loss. If the total angular momentum is nearly independent of color, this indicates that most of the angular momentum came from the core of the main sequence progenitors; current data is consistent with such a conclusion. A larger sample, over a range of color, would enable the relative core and envelope contributions to be better quantified; in fact, such a sample would even be an excellent test for the rotation law enforced in convective regions. For red horizontal-branch stars, which have deep surface convection zones, angular momentum loss from a magnetic wind on the horizontal branch may in addition need to be taken into account in such an analysis.

Models with rotation also need to be evolved from the main sequence to the tip of the giant branch to determine the degree of angular momentum transport from the core to the envelope and to quantify the degree of angular momentum loss on the giant branch. The production of CNO anomalies on the giant branch from rotationally induced mixing will provide a parallel, and important, constraint on the models.

We conclude by noting that the observational database for rotation in metal-poor stars is thin indeed when compared with that for solar-metallicity stars. Even so, these few bits of information have profound consequences for the internal rotation of stars. In this area, as in others, the properties of the oldest stars in the Galaxy have much to teach us about stellar structure and evolution.

We would like to thank A. Boesgaard, D. Duncan, L. Hobbs, R. Noyes, and D. Soderblom for useful discussions about main-sequence rotation velocity measurements in halo stars. This work was supported in part by NASA grant NAGW 778 to Yale University.

REFERENCES

Baglin, A., Morel, P., and Schatzman, E. 1985, *Astr. Ap.*, **149**, 309.
Boesgaard, A. M., and Steigman, G. 1985, *Ann. Rev. Astr. Ap.*, **23**, 319.
Charbonneau, P., and Michaud, G. 1990, *Ap. J.*, **352**, 681.
Deliyannis, C. P., and Pinsonneault, M. H. 1990, *Ap. J. (Letters)*, **365**, 67.
Deliyannis, C. P., Demarque, P., and Pinsonneault, M. H. 1989, *Ap. J. (Letters)*, **347**, L73 (DDP).
Deliyannis, C. P., Pinsonneault, M. H., and Demarque, P. 1990, in preparation.
Demarque, P., and Mengel, J. G. 1971, *Ap. J.*, **164**, 317.
———. 1972, *Ap. J.*, **171**, 583.
Durney, B. R., and Latour, J. 1978, *Geophys. Ap. Fluid Dyn.*, **9**, 241.
Eddington, A. S. 1925, *Observatory*, **48**, 73.
Endal, A. S. 1987, in *The Internal Solar Angular Velocity*, ed. B. Durney and S. Sofia (Dordrecht: Reidel), p. 131.
Endal, A. S., and Sofia, S. 1978, *Ap. J.*, **220**, 279.
———. 1981, *Ap. J.*, **243**, 625.
Faulkner, J. 1966, *Ap. J.*, **144**, 978.
Fox, P. A., and Bernstein, I. B. 1987, in *The Internal Solar Angular Velocity*, ed. B. Durney and S. Sofia (Dordrecht: Reidel), p. 213.
Green, E. M., Demarque, P., and King, C. R. 1987, *The Revised Yale Isochrones and Luminosity Functions* (New Haven: Yale University Observatory).
Green, E. M. 1988, in *Calibration of Stellar Ages*, ed. A. G. Davis Philip (Schenectedy: David Press), p. 81.
Guenther, D. B., Jaffe, A., and Demarque, P. 1989, *Ap. J.*, **345**, 1022.
Harris, W. E., and Racine, R. 1979, *Ann. Rev. Astr. Ap.*, **17**, 241.
Hartmann, L. W., and Stauffer, J. R. 1989, *A.J.*, **97**, 873.
Hartwick, F. D. A., Härm, R., and Schwarzschild, M. 1968, *Ap. J.*, **144**, 978.
Kawaler, S. D. 1987, *Pub. A.S.P.*, **99**, 1322.
———. 1988, *Ap. J.*, **333**, 236.
———. 1989, *Ap. J. (Letters)*, **343**, L45.
Kippenhahn, R., and Möllenhoff, C. 1974, *Ap. Space Sci.*, **31**, 117.
Knobloch, E., and Spruit, H. C. 1982, *Astr. Ap.*, **113**, 261.
Kraft, R. P. 1967, *Ap. J.*, **150**, 551.
Law, W.-Y. 1980, Ph.D. thesis, Yale University.
Lebreton, Y., and Maeder, A. 1986, *Astr. Ap.*, **161**, 119.
Lee, Y.-W., and Demarque, P. 1990, *Ap. J. Suppl.*, **73**, 709.
Lee, Y.-W., Demarque, P., and Zinn, R. 1990, *Ap. J.*, **350**, 155 (LDZ).
Libbrecht, K. G. 1989, *Ap. J.*, **336**, 1092.
Mestel, L., Moss, D. L., and Tayler, R. J. 1988, *M.N.R.A.S.*, **231**, 873.
Noyes, R. W., Hartmann, L. W., Baliunas, S. L., Duncan, D. K., and Vaughan, A. H. 1984, *Ap. J.*, **279**, 763.
Noyes, R. W., Weiss, N. O., and Vaughan, A. H. 1984, *Ap. J.*, **287**, 769.
Pagel, B. E. J., and Simonson, E. A. 1989, to appear in *Rev. Mex. Astr. Ap.*, see Royal Greenwich Observatory preprint 104, 1989 May 12.
Peterson, R. C. 1983, *Ap. J.*, **275**, 737.
———. 1985*a*, *Ap. J.*, **289**, 320.
———. 1985*b*, *Ap. J. (Letters)*, **294**, L35.
Peterson, R. C., Tarbell, T. D., and Carney, B. W. 1983, *Ap. J.*, **265**, 972.
Pinsonneault, M. H. 1988, Ph.D. thesis, Yale University.
Pinsonneault, M. H., and Deliyannis, C. P. 1990, in preparation.
Pinsonneault, M. H., Deliyannis, C. P., and Demarque, P. 1990, in preparation (PDD).
Pinsonneault, M. H., Kawaler, S. D., and Demarque, P. 1990, *Ap. J. Suppl.*, **74**, 501. (PKD).
Pinsonneault, M. H., Kawaler, S. D., Sofia, S., and Demarque, P. 1989, *Ap. J.*, **338**, 424 (PKSD).
Pinsonneault, M. H., and Sofia, S. 1990, in preparation.
Reimers, D. 1975, in *Problems in Stellar Atmospheres and Envelopes*, ed. B. Baschek, W. H. Kagel, and G. Traving (New York: Springer), p. 229.
Rood, R. T. 1970, *Ap. J.*, **161**, 145.
———. 1973, *Ap. J.*, **184**, 815.
Schatzman, E. 1962, *Ann. d'Ap.*, **25**, 18.
———. 1969, *Ap. Letters*, **3**, 139.
Skumanich, A. 1972, *Ap. J.*, **171**, 565.
Smith, G. 1987, *Pub. A.S.P.*, **99**, 67.
Soderblom, D. R. 1990, private communication.
Spruit, H. C. 1987, in *The Internal Solar Angular Velocity*, ed. B. Durney and S. Sofia (Dordrecht: Reidel), p. 185.
Stauffer, J. R., and Hartmann, L. W. 1986, *Pub. A.S.P.*, **98**, 1233.
Suntzeff, N. B. 1989, in *The Abundance Spread within Globular Clusters: Spectroscopy of Individual Stars*, ed. G. Cayrel de Strobel, M. Spite, and T. Lloyd Evans (Paris: Observatoire de Paris), p. 71.
Sweigart, A. V., and Gross, P. G. 1976, *Ap. J. Suppl.*, **32**, 367.
Sweigart, A. V., and Mengel, J. G. 1979, *Ap. J.*, **229**, 624.
Tassoul, J.-L. 1978, *Theory of Rotating Stars* (Princeton: Princeton University Press).
Tassoul, M., and Tassoul, J.-L. 1982, *Ap. J. Suppl.*, **49**, 317.

Tassoul, M., and Tassoul, J.-L. 1989, *Ap. J.*, **345**, 472.
Vauclair, S. 1988, *Ap. J.*, **335**, 971.
Zahn, J.-P. 1983, in *Astrophysical Processes in Upper Main-Sequence Stars*, ed. A. N. Cox, S. Vauclair, and J.-P. Zahn (Geneva: Publ. Observatoire Genève), p. 253.
Zahn, J.-P. 1987, in *The Internal Solar Angular Velocity*, ed. B. Durney and S. Sofia (Dordrecht: Reidel), p. 201.
Zinn, R., and West, M. 1984, *Ap. J. Suppl.*, **55**, 45.

Note added in proof.—(1) Groombridge 1830 has a measured $v \sin i$ of 1.0 ± 1.0 km s^{-1} (M. Smith, *Ap. J.*, **224**, 584 [1978]); we thank S. Ryan for pointing this out. (2) S. Ryan and C. Deliyannis have recently observed some halo dwarfs at high resolution (~ 3 km^{-1}); a *preliminary* assessment indicates no strong evidence for rotational broadening.

CONSTANTINE P. DELIYANNIS, PIERRE DEMARQUE, and MARC H. PINSONNEAULT: Center for Solar and Space Research, Yale University, P.O. Box 6666, New Haven, CT 06511